

# Exploring the mechanism of Xihuangwan on oral squamous carcinoma through network pharmacology, molecular docking and experimental validation

*Running title: XHW: Unraveling the OSCC Treatment Potential*

Xia Luo<sup>1</sup>, Cancan Meng<sup>1</sup>, Mingyang Li<sup>1</sup>, Dongsheng Zhang<sup>2\*</sup>

<sup>1</sup>Department of Oral and Maxillofacial Surgery, Shandong University, Jinan 250000, Shandong, China

<sup>2</sup>Department of Oral and Maxillofacial Surgery, Shandong Provincial Hospital Affiliated to Shandong First Medical University, Jinan 250000, Shandong, China

\*Corresponding author Email : ds63zhang@163.com

## Found

Natural Science Foundation of Shandong Province, China+ZR2021MH353, Dongsheng Zhang

Natural Science Foundation of Shandong Province, China+Grant No. ZR2020QH157, Xuan Wang

## Abstract

**Background:** Oral squamous cell carcinoma (OSCC) is a prevalent and aggressive form of oral cancer that significantly impacts patient quality of life. Xihuangwan (XHW), a traditional Chinese medicine formula, has shown potential in treating OSCC, but the mechanisms underlying its therapeutic effects remain unclear. This study aims to explore the pharmacological mechanisms of XHW in OSCC treatment using network pharmacology, molecular docking, and experimental validation.

**Methods:** We identified key chemical components of XHW and their targets from the BATMAN-TCM database and gathered OSCC-related targets from Gencards,

OMIM, TTD, and DRUGBANK. A compound-target-OSCC system was constructed, and GO and KEGG enrichment analyses were performed. Molecular docking was conducted, followed by experimental validation using cellular experiments.

**Results:** The study revealed key ingredients in XHW, such as estradiol, androstenedione, cholic acid, deoxycholic acid, and dihydroxybenzoic acid, which target core proteins like TNF, ESR1, PTGS2, PPARG, NR3C1, and CAT in OSCC. XHW was found to influence pathways related to tumors, carcinogenesis, endocrine and metabolism, inflammation, and the immune system. Molecular docking confirmed strong bindings between XHW components and core targets. Cellular experiments validated XHW's inhibitory effect on proliferation and its ability to induce apoptosis in CAL27 cells, along with the modulation of key protein mRNA expression levels.

**Conclusion:** This study provides initial insights into the multifaceted mechanisms of XHW in treating OSCC, involving various components, targets, and pathways. The findings suggest the potential of XHW as a multicomponent, multi-target therapeutic agent for OSCC treatment and set the stage for further clinical development and application.

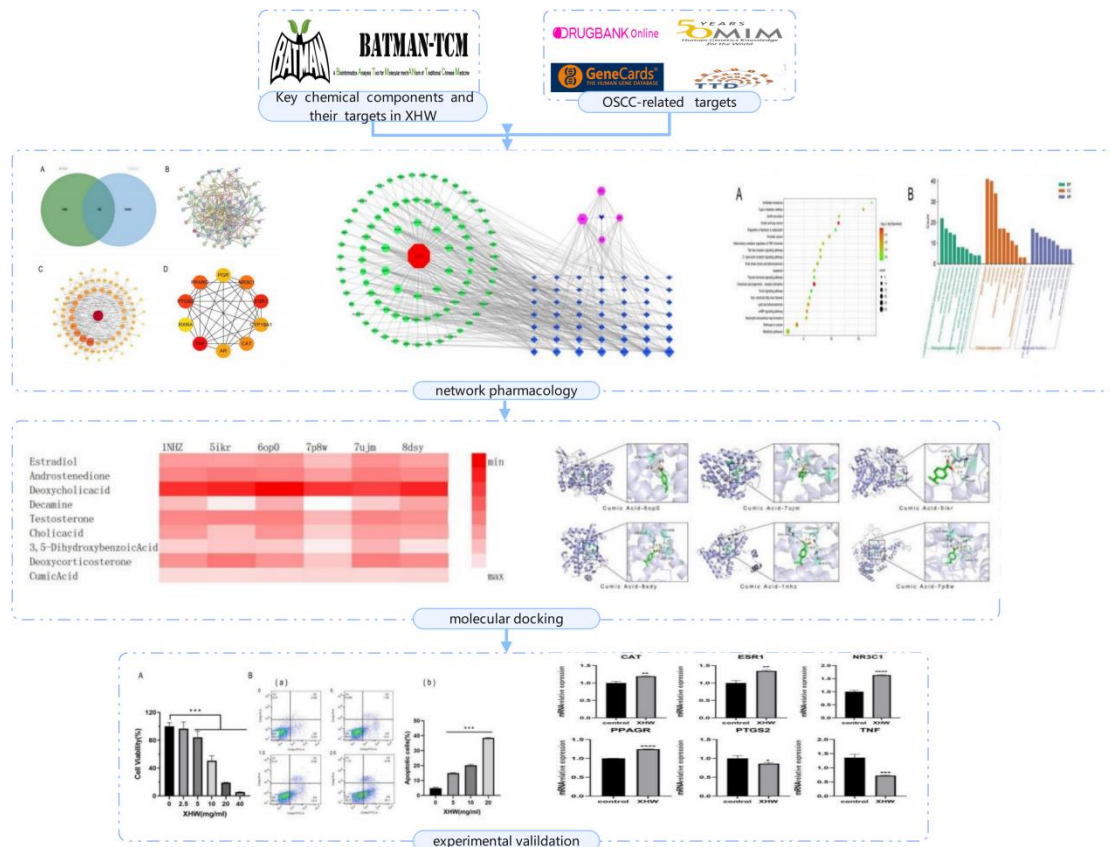
### **Highlight**

Our study uncovers the multifaceted mechanisms of XHW in treating oral squamous cell carcinoma (OSCC), bridging traditional Chinese medicine with modern pharmacological approaches. Through network pharmacology and molecular docking techniques, we identified key active components in Xihuangwan (XHW) that play a crucial role in the treatment of oral squamous cell carcinoma (OSCC), including estradiol, androstenedione, cholic acid, deoxycholic acid, and 3,5-dihydroxybenzoic acid. We have identified core targets such as TNF, ESR1, PTGS2, PPARG, NR3C1,

and CAT, which are crucial in the pharmacological action of XHW on OSCC. XHW is shown to influence various pathways related to tumors, carcinogenesis, endocrine and metabolism, inflammation, and the immune system in OSCC. Molecular docking studies confirm strong binding between XHW's core targets and its components, suggesting potential therapeutic efficacy. Cellular experiments validate XHW's inhibitory effect on proliferation and its ability to induce apoptosis in CAL27 cells, along with the modulation of key protein mRNA expression levels. The findings provide a foundation for the clinical development and application of XHW in OSCC treatment, highlighting its multicomponent, multi-target therapeutic potential.

**Keywords:** Xihuangwan; oral squamous cell carcinoma; network pharmacology; molecular docking; in vitro experiments.

### **Graphical abstract**



## 1. Introduction

Oral squamous cell carcinoma (OSCC) is a highly aggressive head and neck tumour, constituting approximately 90% of oral cancer cases<sup>1</sup>. It significantly impairs speech, mastication, and swallowing, negatively impacting patients' appearance and mental well-being. OSCC significantly diminishes patients' quality of life and places a heavy financial strain on society<sup>2</sup>. In China, the oral cancer incidence rate is about 3.78 per 100,000, with approximately 52,000 new cases and 26,000 deaths annually<sup>3</sup>. While early-stage oral cancer is often treatable with extensive surgical resection, intermediate and late-stage OSCC, particularly in recurrent cases, present greater challenges.

With the robust growth of Traditional Chinese Medicine (TCM) in recent years, its potential advantages in tumor treatment have become increasingly evident. TCM has the potential to complement Western medicine by enhancing efficacy and reducing toxicity, thereby ameliorating clinical symptoms in

patients with middle and advanced stage tumors and enhancing their overall quality of life<sup>4</sup>

## **2. Materials and methods**

### **2.1 Purchasing XHW's Active Ingredients and Targets**

We examined the compounds and their targets among the four elements of XHW's traditional Chinese medicine—Calculus bovis, Musk, Frankincense, and Myrrh—using the BATMAN-TCM database<sup>14</sup>. Employing "SHE XIANG," "NIU HUANG," "RU XIANG," and "MO YAO" as search terms, we adjusted the parameters to "Score cutoff=80" and "Adjusted P-value=0.05."<sup>8</sup> Stringent measures were applied to eliminate duplicate targets. Furthermore, we expanded the dataset with known targets linked to unexpected active compounds, as documented in the existing literature.

### **2.2 Screening Targets for Oral Squamous Cell Carcinoma**

We performed target screening for OSCC utilising the GeneCards, OMIM, and TTD databases. The term "oral squamous cell carcinoma" was used to identify disease-related target genes, which were then standardized and compiled into an Excel table. We utilized the DRUGBANK database to identify action targets of first-line Western drugs for OSCC treatment<sup>15</sup>. A higher score in the GeneCards database indicates a closer connection to the condition. Our methodology involves selecting potential OSCC targets by setting a threshold at the median Score value when dealing with an extensive list of targets. Subsequently, we eliminated duplicate entries among the four targets in the disease database to refine our list of OSCC targets.

### **2.3 Identification intersecting targets of XHW and OSCC**

We collected targets associated with both XHW and OSCC, and subsequently uploaded them to the online cloud platform for bioinformatics analysis and visualization, Bioinformatics ( <https://www.bioinformatics.com.cn/>). Utilizing Venn diagrams, we identified common targets by intersecting the two sets.

## 2.4 Creation of the PPI Network Including the OSCC and XHW Components'

### Targets

We developed a PPI network model to clarify the interactions between drug targets in XHW and OSCC-associated targets. The STRING 12.0 database was updated with the common targets under the biological species "Homo sapiens". We established a minimum interaction threshold of "medium confidence" ( $>0.4$ ). Other settings were maintained as defaults to generate the PPI network schematic.

## 2.5 Construction of target-active compound network

With the use of Cytoscape 3.9.1, we visualized the complex interactions among XHW Pills, their traditional Chinese medicine components, active ingredients, targets, and OSCC, termed 'Xihuang Pills - Traditional Chinese Medicines - Active Ingredients - Targets - OSCC'. The main active elements that cause pharmacological effects were examined using the built-in tools, which include Degree, Betweenness, and Closeness.

## 2.6 Examination of KEGG Pathways and GO Enrichment

To acquire GO and KEGG data, we used the DAVID database (<https://david.ncifcrf.gov/>). GO analysis facilitated the identification of molecular functions (MF), biological processes (BP), and cellular components (CC)<sup>16</sup>. KEGG enrichment analysis revealed key signaling pathways associated with these biological processes. The Bioinformatics platform (<http://www.bioinformatics.com.cn/>) received the Gene Ontology and KEGG data

for visual analysis. The GO analysis results were shown as bar charts, while the KEGG pathway enrichment results were displayed as bubble charts.

## 2.7 Molecular Docking Validation

We selected the receptor because to its high ranking in the PPI network and chose ligands from active components with top-degree rankings in the Traditional Chinese Medicine (TCM) compound-target network for binding energy predictions. A lower binding energy value indicates stronger binding capability. We retrieved the Uniprot IDs for the target proteins by entering their gene names into the Uniprot database (<https://www.uniprot.org/>). UniProt IDs were utilized to obtain the three-dimensional models of target proteins from the RCSB PDB database (<http://www.rcsb.org/>) and preserved in PDB format. The files were later imported into PyMOL 310 program for additional processing, including dehydration and ligand removal operations. Following initial preparation, the refined pdb files were introduced into AutoDockTools 1.5.7 for hydrogenation, designated as receptors, then exported as pdbqt files. The active chemicals' three-dimensional structures were obtained from the PubChem database and stored in sdf format. To simplify further processes, we utilized OpenBabel 2.4.1 to change the files' format to Mol2. Using AutoDockTools 1.5.7, we performed hydrogenation, configured the ligands, identified torsional bonds, and saved the files in pdbqt format for export. The pdbqt format ligand and receptor files were brought into AutoDockTools 1.5.7 for semi-flexible docking analyses. PyMOL was used to visualise the outcomes of this docking research.

## 2.8 In vitro experimental validation

### 2.8.1 Primary Materials

The traditional Chinese medicine formula XHW was acquired from Beijing Tong Ren Tang Development Co., Ltd (Batch No.: Z11020073). CAL27 human tongue squamous cell carcinoma cells were provided by our laboratory. DMEM

medium was obtained from Corning Corporation. Fetal bovine serum (FBS) was purchased from Ausbian Corporation in Australia. The CCK-8 reagent kit and Giemsa stain solution were procured from Sigma Corporation in the US. The Beyotime Corporation provided the Annexin V-FITC/PI Apoptosis Detection kit. The 5 × Evo M-MLV reverse transcription reagent premix (Batch number: A5A043, Huanan Aikerui Biotechnology Co., Ltd) and SYBY Green Pro Taq HS pre-mixed qPCR reagent kit (Batch number: A5A0189, Huanan Aikerui Biotechnology Co., Ltd) were also used.

## 2.8.2 Methodology

### 2.8.2.1 Preparation of Chinese Herbal Medicine Extracts

XHW was immersed in pre-cooled distilled water at 4 °C with a concentration of 0.1 g/mL in a sterile, airtight container for 24 hours. After 2 hours of ultrasonic oscillation, the mixture was soaked at 4 °C for an additional 48 hours. The supernatant underwent two rounds of centrifugation at 15,000 r/min for 15 minutes and was filtered to produce the XHW extract using a 0.22 µm microporous filter, which was kept for later use at 4 °C or -20 °C.

### 2.8.2.2 Cell Culture

Following resuscitation, CAL27 cells were kept in DMEM with 1% penicillin and 10% foetal bovine serum added. The culture flasks were placed in a 37°C, 5% CO<sub>2</sub> incubator, and the culture fluid was replaced every two days. Cells were examined microscopically, and upon reaching 70%–80% confluence, they were digested with trypsin-EDTA and passaged.

### 2.8.2.3 CCK-8 assay for cell proliferation

Cells were divided into control group (no drug added) and experimental group (2.5, 5, 10, 20、40 g-L<sup>-1</sup>). The cells were inoculated in 96-well plates, and 5 replicate wells were set in each group.



#### 2.8.2.4 Apoptosis Rate Detection via Flow Cytometry

Three duplicates of Cal27 cells were planted into a 6-well plate. Cells adhered to the wall were cultured for 48 hours with varying concentrations (0, 5, 10, 20 g-L-1) of Xihuangwan extract. Post-culture, the cells were digested using EDTA-free trypsin, followed by centrifugation and collection. Add AnnexinV-FITC to Cal27 cells, then add AnnexinV-FITC and PI and mix well, and incubate away from light. Cell apoptosis in each group was assessed using flow cytometry.

#### 2.8.2.5 RT-PCR Analysis of TNF, ESR1, PTGS2, PPARG, NR3C1, and CAT mRNA Expression Levels<sup>17, 18</sup>.

The cells were rinsed with PBS, and lysate was added. After centrifugation to collect RNA precipitate, RNA concentration and integrity were assessed. The RNA was reverse-transcribed into cDNA for amplification, utilising GAPDH as the internal reference. We utilized the 2- $\Delta\Delta C_t$  method for target gene expression analysis, with primer sequences detailed in Table 1.

**Table 1** Primer Design for Quantitative Real-Time Polymerase Chain Reaction

Primer name	Primer sequence (5'to3')	Primer length
TNF-F (Homo)	CTGCCTGCTGCACTTTGGAG	20
TNF-R (Homo)	ACATGGGCTACAGGCTTGTCA	21
ESR1-F (Homo)	CGATGATGGGCTTACTGACCAA	22
ESR1-R (Homo)	AGGATCTCTAGCCAGGCACATTC	23
PTGS2-F (Homo)	CCAGCACTTCACGCATCAGTT	21
PTGS2-R (Homo)	TGTCTAGCCAGAGTTTCACCGTAA	24
PPARG-F (Homo)	CACATTACGAAGACATTCCATTAC	25
PPARG-R (Homo)	GGAGATGCAGGCTCCACTTTG	21

NR3C1-F (Homo)	CAGGCTGGAATGAACCTGGAA	21
NR3C1-R (Homo)	GTTCAATAACCTCCAACAGTGACA	24
CAT-F (Homo)	TCATCCAGAAGAAAGCGGTCAA	22
CAT-R (Homo)	TCAGCATTGTACTTGTCCAGAAGA	24

---

### 2.8.2.6 Analysis of Statistics

With SPSS 22.0, statistical analysis was carried out. Each group's information were subjected to normality and chi-square tests. For multigroup comparisons, a one-way ANOVA was employed, with a significance level of  $P < 0.05$ .

## 3. Results

### 3.1 Obtaining Active Ingredients and Targets of XHW

After de-weighting, we retrieved a total of 49 primary active ingredients and identified 270 gene targets for XHW using the BATMAN-TCM database. We extracted the two primary constituents and their corresponding two principal targets from the database, which are summarized in Table 2. Musk, for instance, comprises 19 active ingredients and is associated with 175 gene targets. Calculus bovis includes 8 active ingredients and has 90 gene targets, frankincense encompasses 13 active ingredients connected to 119 gene targets, while myrrh has 9 active ingredients associated with 74 gene targets.

**Table 2** Compilation of Pharmaceutical Ingredients and Targets for Xihuang Pills

Pharmaceutical nomenclature	Active ingredient	Targets						
Musk	Androst-4-Ene-3,17-Dione	CYP17A1	AR	RYR1	PRKDC	ADORA2B	PDE1B	
		PDE10A	PDE2A	HDAC2	ESR1	PDE7B	PDE3A	PIK3CD
		PDE1A	PDE7A	PDE1C	ADORA1		PDE6C	PGR
		PDE5A	ADORA2A		PDE3B	PDE4D	ITPR3	ATM
		CYP19A1		PDE11A	OPRK1	PDE9A	ITPR1	PGD
		PIK3CB	POLA2	PDE6B	PDE8B	PDE8A	NR3C2	PDE4A

		PDE6A	PIK3CA	ITPR2	PDE4C	PDE4B	NT5E	
Musk	Testosterone	AR	NR3C1	SRD5A1	OPRK1	CYP17A1		ANXA1
		ESR1	NR3C2	PGR	ATP1A1			
		SCN11A	SCN3B	SCN3A	AKR1D1	AR	PLA2G1B	
		SCN4B	SRD5A2	COX2	ADH1A	SCN2B	COX6C	AKR1C2
		ALDH5A1		COX7A1	COX6A2	ADH1C	ACADSB	
		OGDH	ADH1B	ABAT	COX5B	SCN7A	SCN2A	FECH
Calculus bovis	Deoxycholic acid	TYR	COX6B1	SCN8A	HDAC2	AKR1C1	SCN1A	COX7C
		SCN5A	COX5A	COX4I1	SCN9A	FABP6	COX7B	COX8A
		ESRRG	COX1	SCN10A	COX3	HDAC9	SCN4A	CES1
		SCN1B	NR1H4					
Calculus bovis	choline	PLD1	PLD2	PCYT1A	BCHE	PCYT1B	PHOSPHO1	
		ACHE						
Frankincense	Octyl acetate	NPR1						
Frankincense	Phellandral	CYP17A1	NR3C2	ESR1	ACHE	PGR	BCHE	AR
		OPRK1						
Myrrh	cumic acid	PLAT	BCL2	PTGS2	HCAR2	FABP2	NNMT	THBD
		CFTR	PPARG	HCAR3	QPRT	PTGS1		
Myrrh	Commiferin	HMGCR	ITGB2	ITGAL	HDAC2			

### 3.2 Identification of OSCC-Related Targets

From the Genecards database, we identified 6,729 OSCC-related targets and selected potential targets with a Score above the median. For instance, the Score values for OSCC targets obtained from GeneCards ranged from a minimum of 0.7274911 to a maximum of 449.3358765, with a median of 14.455508. Therefore, any target with a Score greater than 14.455508 was designated as a potential OSCC target. We supplemented these targets by cross-referencing data from the OMIM, TTD, and DRUGBANK databases, removing duplicates in the process, resulting in a final compilation of 3575 OSCC-related targets.

### 3.3 Acquisition of XHW component-OSCC related targets

We imported the 270 targets associated with XHW and the 3575 targets related to OSCC into the online bioinformatics analysis and visualization platform (bioinformatics.com.cn). From this analysis, we identified 85 intersecting targets between the drug (XHW) and the disease (OSCC), as illustrated in Figure 1A. The list of these intersecting targets can be found in Table 3. These intersecting targets represent the specific targets of XHW in the management of OSCC.

**Table 3** List of Overlapping Targets Between Xihuang Pills and OSCC

Serial number	Targets	Serial number	Targets	Serial number	Targets
1	CYP17A1	30	SLC6A3	59	NR1H4
2	AR	31	PTGER4	60	VDR
3	PRKDC	32	ESR2	61	CYP27B1
4	HDAC2	33	DRD4	62	TRPV3
5	ESR1	34	DRD2	63	ADH1B
6	PIK3CD	35	ESRRB	64	SCN5A
7	PGR	36	NOS2	65	HDAC9
8	ATM	37	NR0B1	66	ACHE
9	CYP <sup>19</sup> A1	38	GRIN1	67	MPL
10	ITPR1	39	GRIN2B	68	CAT
11	PIK3CB	40	F2	69	ALDH2
12	NR3C2	41	HTR2A	70	TPO
13	PDE4A	42	TLR8	71	CACNA1G
14	PIK3CA	43	TLR7	72	TNF
15	NT5E	44	ADRB2	73	TOP1
16	ANXA1	45	PRKAA1	74	RBP1
17	ATP1A1	46	CYP2B6	75	ALDH1A1
18	PTGS1	47	AGTR1	76	PLAT
19	PTGS2	48	MTAP	77	BCL2
20	PPARG	49	ACP1	78	NNMT
21	ALOX5	50	PROS1	79	THBD
22	MPO	51	DHFR	80	CFTR

23	IKBKB	52	CACNA1C	81	HMGCR
24	AKR1C1	53	TYMS	82	ITGB2
25	CHUK	54	TYR	83	ITGAL
26	PTGER2	55	SRD5A2	84	RXRB
27	NR3C1	56	FECH	85	RXRA
28	SRD5A1	57	ADH1C		
29	NR1H2	58	COX5A		

---

### 3.4 Development and Examination of the PPI Network

To create a PPI network model, the 85 OSCC targets of XHW were added to the STRING12.0 database. The biological species was designated as "Homo sapiens," and the minimal interaction threshold was set at "medium confidence" ( $>0.4$ ). As shown in Figure 1B, the PPI network was obtained by deleting free nodes while maintaining the remaining settings at their default levels. With 382 edges and 84 nodes, the network has a local clustering coefficient of 0.459 and an average node degree of 9.1. In the diagram, nodes denote proteins, while edges indicate the interactions between them. The greater the number of edges between two nodes and the darker their color, the stronger the correlation. The results were visualized using CytoScape3.9.1, shown in Fig. 1C. Network topology parameters were analysed using the built-in tools of CytoScape 3.9.1, including Degree of Connectivity, Betweenness, and Closeness, to identify core treatment targets. The ten highest-ranked objectives by Degree were designated as core targets, as illustrated in Fig. 1D. This suggests that TNF, ESR1, PTGS2, PPARG, NR3C1, CAT, and others could be core targets for XHW in treating OSCC. The network topology parameters for each core target are presented in Table 4.

### 3.5 Construction of the XHW Active Component-OSCC Targets Network

Making use of CytoScape 3.9.1, we constructed a network diagram depicting XHW, its herbal medicine components, active ingredients, associated targets, and OSCC, as shown in Fig.2. We examined network topology characteristics for active components and targets using the built-in capabilities in CytoScape 3.9.2. This analysis, which comprises the degree of connection, betweenness, closeness, and average shortest path length, allowed us to identify the primary active ingredients responsible for the pharmacological effects based on their network topology. Table 5 lists the top 12 Degree active ingredients and its parameter values.

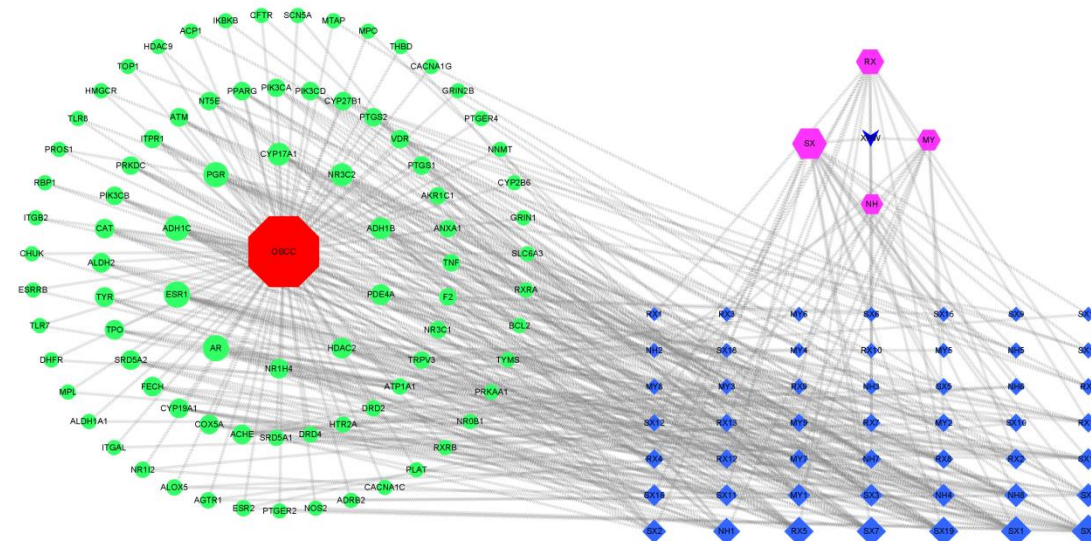


**Fig. 2.** Network Diagram of Xihuang Pills - Traditional Chinese Medicine - Active Ingredients - Targeted Actions - OSCC

**Table 5** Top 10 Active Ingredients in Xihuang Pills for the Treatment of OSCC by Degree Value Ranking

Active Ingredient	chemical name	Degree	AverageShortestPathLength	Betweenness	ClosenessCentrality
SX4	17-Beta-Estradiol	19	2.669064748	0.02356158	0.374663073
SX1	Androst-4-Ene-3,17-Dione	16	2.712230216	0.010828822	0.368700265
SX19	5-Cis-Cyclotetradecen-1-One	15	2.755395683	0.008163621	0.362924282

SX7	5-Cis-Cyclopentadecen-1-One	15	2.755395683	0.008163621	0.362924282
RX5	P-Menth-4-En-3-One	15	2.784172662	0.014189707	0.359173127
NH1	Deoxycholicacid	13	2.784172662	0.011921184	0.359173127
SX8	Decamine	10	2.899280576	0.008724553	0.344913151
SX2	Testosterone	10	2.798561151	0.007307279	0.357326478
NH8	Cholicacid	10	2.884892086	0.006584496	0.346633416
SX3	3,5-Dihydroxybenzoic Acid	9	2.856115108	0.008670259	0.350125945
NH4	Deoxycorticosterone	9	2.899280576	0.006670001	0.344913151
MY1	Cumic Acid	9	3.043165468	0.007951197	0.328605201

---

### 3.6 KEGG Pathway and GO Enrichment Analysis

Through an analysis of intersecting genes using the DAVID database, we identified 277 items related to Biological Process (BP) in the GO functional enrichment analysis. The processes involved included responses to foreign biological stimuli, intracellular steroid hormone receptor signaling, inflammatory responses, and favorable control of the vitamin D receptor signaling pathway and the transcription of the RNA polymerase II promoter. For Cellular Component (CC), 53 items were identified, such as the cell surface, receptor complexes, chromatin, endoplasmic reticulum membrane, and plasma membrane. In terms of Molecular Function (MF), 102 items were noted, including the estrogen response, ligand activation, sequence-specific DNA binding, and RNA polymerase II transcription factor activity. The top ten products in the BP, CC, and MF categories were ranked by P-values and visualized as bar graphs in Fig.3A. In the examination of KEGG pathway enrichment, we determined 79 signaling pathways, which were ranked according to their P-values, with the top 20 pathways depicted in bubble plots, as shown in Fig.3B. The top 20 enriched pathways include small cell lung cancer, chemical carcinogenesis-receptor activation, cancer pathways, prostate cancer, type 2 diabetes mellitus, fluid shear stress and atherosclerosis, lipids and atherosclerosis, cAMP signaling, GnRH secretion, metabolic pathways, inflammatory mediator

modulation of tryptophan channels, cell apoptosis, C-type lectin receptor signaling, neutrophil extracellular trap formation, Toll-like receptor signaling, nonalcoholic fatty liver disease, regulation of lipolysis in adipocytes, thyroid hormone signaling, antifolates, and the FoxO signaling pathway.

### 3.8 In vitro experimental validation

#### 3.8.2.3 Assay for CCK-8

When compared to the control group (0 g/L), the CCK-8 test showed that XHW substantially suppressed CAI27 cell growth in a dose-dependent manner at doses of 2.5, 5, 10, 20, and 40 g/L, as shown in Figure 6A. To explore the underlying mechanisms, subsequent experiments were conducted using XHW concentrations of 0, 10, and 20 g/L on CAI27 cells after calculating the IC<sub>50</sub> values for inhibiting cell proliferation.

#### 3.8.2.4 Determination of Apoptosis Rate Using Flow Cytometry

At doses of 5, 10, and 20 g/L, the Annexin V-FITC/PI double labeling experiment showed that XHW caused apoptosis in CAI27 cells in a concentration-dependent manner in contrast to the control group (0 g/L) (see Figure 6B).

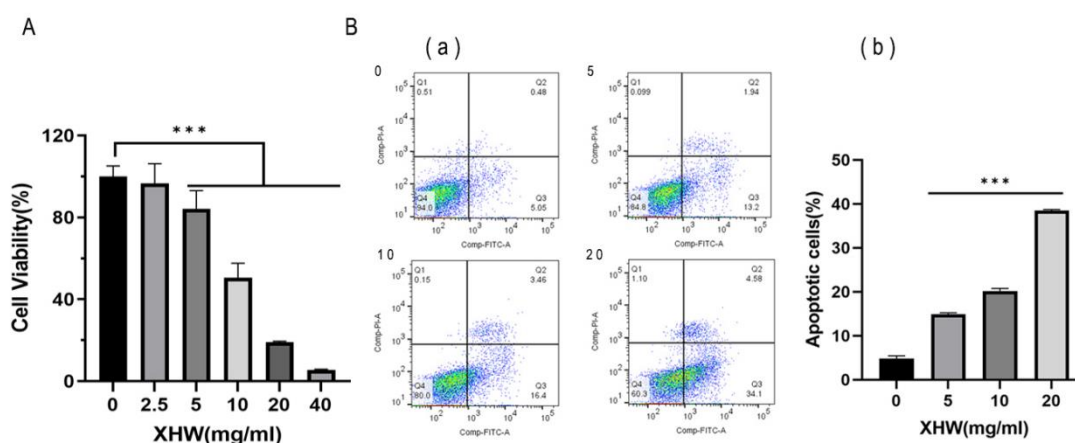




**Fig. 6. A** With the increase of xhw concentration, the proliferation rate of Cal27cells gradually decreased. Compared with the control group, \*\*\*P<0.001. **B** XHW significantly promoted apoptosis

of HemEC cells. (a). Flow cytometry; (b). Cell apoptosis rates. Compared with the control group, \*\*\*P<0.001.

### 3.8.2.5 RT-PCR Analysis of TNF, ESR1, PTGS2, PPARG, NR3C1, and CAT mRNA Expression Levels

XHW intervention significantly increased mRNA expression of ESR1, PPARG, NR3C1, and CAT proteins in CAL27 cells (P<0.05). When compared to the blank group, the TNF and PTGS2 protein mRNA expression levels were considerably lower (P<0.05). For a graphic depiction of the results, see Figure 7.

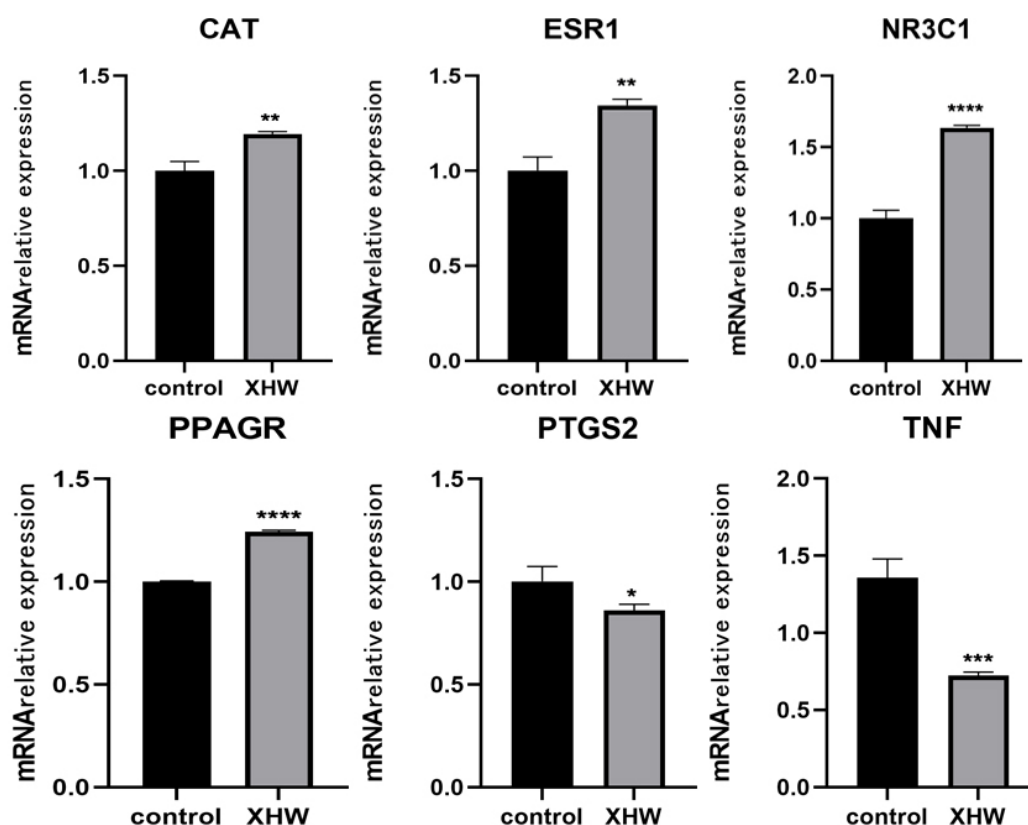


**Fig. 7.** Effect of XHW on the relative mRNA expression of core targets, \*P<0.05, \*\*P<0.005, \*\*\*P<0.001, \*\*\*\*P<0.0001.

#### 4. Discussion

This study uses network pharmacology, in vitro assays, and molecular docking to clarify how XHW works to treat oral squamous cell carcinoma (OSCC). The results reveal that XHW's efficacy in OSCC treatment is mainly due to active ingredients such as steroid hormones, including estradiol, 11-deoxycorticosterone, and androstenedione. Additionally, Cholic acid, Deoxycholic acid, and 3,5-Dihydroxybenzoic Acid are involved in lipid metabolism, while Cumic Acid is recognized for its antimicrobial and antitumor properties.

Patients suffering from severe illnesses, such as advanced cancer, display a pronounced hyperinflammatory response characterized by the emergence of cytokine storm syndrome, heightened coagulation tendencies, and compromised cell-mediated immunity<sup>20</sup>. High amounts of circulating cytokines and excessive immune cell activation are hallmarks of severe systemic inflammatory diseases such as cancer-induced cytokine storm and cytokine release syndrome (CRS)<sup>21</sup>. These conditions often involve tumor microenvironment immunosuppression<sup>22, 23</sup>. Sex steroids, with their notable immunomodulatory effects, can influence immune responses and disease-related inflammation due to differing levels of estrogen, progesterone, and androgens between females and males<sup>24</sup>. Increased physiological levels of progesterone (P4) and 17 $\beta$ -estradiol (E2) have anti-inflammatory and immunomodulatory properties<sup>25-27</sup>. In severe and acute conditions like advanced cancer, the hypothalamic-pituitary-gonadal axis may be disrupted, reducing endogenous E2 and P4 production<sup>24</sup>. Moreover, hormones present promising prospects for

therapeutic interventions<sup>20</sup>. Numerous immune cells include estrogen receptors (ERs), is operated as transcriptional regulators of cellular activity<sup>28</sup>. In both human and animal models, 17 $\beta$ -estradiol (E2) treatment has shown beneficial immunomodulatory and anti-inflammatory benefits when blood concentrations are comparable to those seen during ovulation or pregnancy<sup>29</sup>. Increased E2 levels prevent neutrophil and monocyte migration to inflammatory regions by suppressing pro-inflammatory cytokines in macrophages, such as TNF- $\alpha$ , IL-6, IL-1 $\beta$ , and CCL2<sup>30</sup>. This aligns with our PCR findings of low TNF target gene expression and high ESR1 expression. 11-Deoxycorticosterone, a salt corticosteroid, is hydroxyl-substituted at position 21 and functionally related to luteinizing hormone<sup>31</sup>. Progesterone (P4) inhibits macrophages and dendritic cells from producing proinflammatory cytokines including IL-1 $\beta$  and interleukin 12. Elevated E2 and P4 levels enhance anti-inflammatory cytokine production, such as interleukin 4 and interleukin 10, by CD4+ T helper cells, promoting a Th2-type response<sup>32</sup>. These hormones likely synergize to reduce pro-inflammatory cytokine production by innate immune cells, promoting T cell immunological tolerance, B cell generation of more antibodies, and anti-inflammatory reactions<sup>24</sup>. We propose that short-term E2 and P4 treatment may improve B-cell responses and antibody production while inhibiting the innate immunological inflammatory response, potentially serving as a promising treatment for advanced OSCC patients with minimal side effects when using XHW. As fatty acid-activated transcription factors that control energy metabolism, peroxisome proliferator-activated receptors (PPARs) are a subfamily of nuclear hormone receptors. They are associated with a wide range of human illnesses, including cancer<sup>33-35</sup>, autoimmune conditions<sup>36</sup>, metabolic disorders, and comprise three isoforms: PPAR $\alpha$ , PPAR $\beta/\delta$ , and PPAR $\gamma$  (PPARG). PPARG expression products have a role in immune-mediated inflammatory disorders and are essential for both innate and adaptive immune system functioning<sup>37</sup>.

Furthermore, PPARG is significant for adipose tissue development, lipid metabolism, and energy homeostasis<sup>38</sup>. Glucocorticoids find application in treating inflammatory diseases, autoimmune conditions, and certain cancers<sup>39</sup>. Their anti-inflammatory and anti-tumor effects are partially ascribed to glucocorticoid-induced apoptosis. When glucocorticoids attach to the glucocorticoid receptor (GR), pro-apoptotic genes are upregulated and anti-apoptotic genes are downregulated<sup>40</sup>. PTGS2 is the primary isoenzyme responsible for synthesizing inflammatory prostaglandins and holds a pivotal role in pathologies linked to inflammatory signaling<sup>41</sup>. CAT converts hydrogen peroxide produced by peroxidases into water and oxygen, protecting cells from toxicity. Additionally, CAT promotes cell growth, including T-cells and B-cells<sup>42</sup>. PCR experiments have shown a high expression of PPARG, NR3C1, and CAT, and a low expression of PTGS2, confirming previous findings. Androstenedione, a steroid hormone generated in both sexes' gonads and adrenal glands, plays a crucial role in estrogen and testosterone synthesis. It is believed that raising testosterone levels will boost sexual performance, maintain healthy red blood cells, reduce fat, promote muscular building, and improve athletic ability<sup>43</sup>. Androstenedione raises the levels of estradiol while lowering triglycerides (TG) and high-density lipoprotein (HDL) cholesterol<sup>44</sup>.

One notable metabolic disturbance in cancer is aberrant lipid metabolism. Lipid metabolism is necessary for cancer cells to produce energy, build critical biofilm components, and synthesize signaling chemicals that are necessary for invasion, metastasis, proliferation, survival, adaptability to the tumor microenvironment, and cancer treatment<sup>45</sup>. Bile acids are essential molecules for lipid absorption and cholesterol regulation, significantly influencing glucose control and energy balance. The bile acid pool comprises main bile acids, including cholic acid (CA) and chenodeoxycholic acid (CDCA), which are generated from cholesterol in the liver.

It comprises secondary bile acids altered by intestinal bacteria, including deoxycholic acid (DCA), lithocholic acid (LCA), and ursodeoxycholic acid (UDCA)<sup>46</sup>. Intestinal bacteria transform deoxycholic acid, a secondary bile acid, into ursodeoxycholic acid, which is essential for preserving the integrity of the intestinal barrier and promoting lipid metabolism. UDCA has both pro- and anti-apoptotic effects on different cell types, depending on the situation. In addition to preventing cancer cell development and triggering apoptosis or autophagic cell death, UDCA drugs shield epithelial cells from harm and apoptosis. Additionally, the UDCA protects against harm from cancer chemotherapeutic treatments by influencing tumor cell migration, tumor stem cells, and ecological dysregulation brought on by medications<sup>47</sup>. Stimulation of hydroxybenzoic acid receptors by 3,5-Dihydroxybenzoic Acid leads to a decrease in adipocyte lipolysis, potentially benefiting the lipid profile<sup>48</sup>. Furthermore, 3,5-DHBA's effects, which are mediated by HCAR1, have important ramifications for the neurological system, stem cell maintenance, the regulation of carcinogenesis, and the reaction to anticancer therapies—presenting both benefits and threats to human health<sup>49</sup>.

Decamine, a broad-spectrum antibiotic, has been clinically validated for its remarkable safety profile. Recent investigations have revealed its potential in restraining malignant tumor growth, owing to its unique capacity to accumulate within mitochondria, resulting in effective tumor cell growth inhibition<sup>50</sup>. Furthermore, Decamine serves as an inhibitor of XIAP, acting as a mitochondria-targeting agent, thus offering intriguing insights into cutting-edge approaches to tumor therapy<sup>51</sup>. On the other hand, Cumic Acid demonstrates antifungal properties<sup>52</sup>, while its derivatives have antimicrobial and antibacterial effects<sup>53</sup>.

We used KEGG and GO to do enrichment studies in order to look into the mechanism of XHW in OSCC. GO analysis identified significant enrichment of target genes in several biological processes, including the positive control of RNA polymerase II promoter transcription, inflammatory response, response to xenobiotic stimuli, and DNA-triggered transcription regulation. KEGG enrichment analysis indicated that XHW influences multiple signaling pathways in OSCC treatment, including those related to tumors, oncology, endocrine and metabolism, inflammation, and the immune system. This finding is consistent with our previous analysis.

Our findings, derived from in vitro tests and molecular docking confirmation, demonstrate that XHW extract effectively suppresses the proliferation, induces apoptosis in CAL27 cells, and modulates the mRNA expression of specific proteins. These experimental findings furnish direct evidence elucidating the molecular mechanisms through which XHW impacts oral squamous carcinoma cells. However, it's crucial to recognize that this study has limits because it only focuses on a few key elements and objectives, without taking into account all other contributing aspects. Furthermore, despite the useful information obtained from cellular in vitro experiments, it is imperative to undertake additional investigations employing animal models and clinical studies to confirm the robustness of these findings within the broader biological context.

Subsequent research endeavors should consider expanding our network pharmacology analysis, encompassing the incorporation of additional targets and pathways. This broader approach will provide a more comprehensive elucidation of XHW's multilevel mechanism of action in the context of oral squamous carcinoma treatment. Furthermore, the amalgamation of animal models and clinical trials can facilitate a more thorough evaluation of both the therapeutic effectiveness and safety profile of XHW. Lastly, exploring

the combined utilization of XHW alongside other therapeutic modalities holds the potential to further augment the therapeutic efficacy for patients afflicted with oral squamous carcinoma.

To sum up, this study provides a preliminary understanding of how XHW works to treat oral squamous cell cancer. This serves as a vital reference point for both its clinical application and future investigations. Nonetheless, further comprehensive research is warranted to enhance our comprehension of its mode of action.

## **5. Conclusion**

In conclusion, this study offers thorough yet early insights into the complex pathways that underlie XHW's therapeutic potential in the treatment of OSCC. XHW is shown to contain various active ingredients, including sex hormones like estradiol and androstenedione, compounds associated with lipid metabolism such as cholic acid and deoxycholic acid, as well as substances with antimicrobial and antibacterial properties like decamine and cumic acid. The research identifies key targets relevant to OSCC through network pharmacology analysis, including TNF, ESR1, PTGS2, PPARG, NR3C1, and CAT. Additionally, the study uncovers pathways related to processes such as tumorigenesis, carcinogenesis, endocrine regulation, metabolism, inflammation, and immune system modulation, highlighting XHW's multidimensional impact on OSCC. Molecular docking and cellular experiments provide validation for these findings. This study emphasizes the significance of exploring the rich pharmacological landscape of traditional medicine within the modern oncological context, offering promising avenues for innovative cancer therapies.

## Statement of Data Availability

The article and Supplementary Material include the study's unique contributions. For more questions, please contact the corresponding authors.

## Ethics Statement

Participant permission and ethical approval are not relevant for this study because it does not include animal or patient trials.

## Conflicts of interest

No conflicts of interest are disclosed by the writers.

## Author contributions

LUO Xia proposed and designed this work. LUO Xia conducted interpretation and analysis of data, and contributed to write a manuscript. LUO Xia and MENG Cancan performed the cell experiments and data analysis. LUO Xia, LI Mingyang updated the manuscript. The final text has been reviewed and approved by all authors.

## References

- (1) Almangush, A.; Mäkitie, A. A.; Triantafyllou, A.; de Bree, R.; Strojan, P.; Rinaldo, A.; Hernandez-Prera, J. C.; Suárez, C.; Kowalski, L. P.; Ferlito, A.; et al. Staging and grading of oral squamous cell carcinoma: An update. *Oral Oncol.* **2020**, *107*, 6, Review. DOI: 10.1016/j.oraloncology.2020.104799.
- (2) Yang, Y.; Zhou, M. G.; Zeng, X. Y.; Wang, C. X. The burden of oral cancer in China, 1990-2017: an analysis for the Global Burden of Disease, Injuries, and Risk Factors Study 2017. *BMC Oral Health* **2021**, *21* (1), 11. DOI: 10.1186/s12903-020-01386-y.
- (3) Ghantous, Y.; Abu Elnaaj, I. GLOBAL INCIDENCE AND RISK FACTORS OF ORAL CANCER. *Harefuah* **2017**, *156* (10), 645-649, Review.
- (4) Wang, D.; Duan, X. J.; Zhang, Y. H.; Meng, Z.; Wang, J. Traditional Chinese medicine for oral squamous cell carcinoma A Bayesian network meta-analysis protocol. *Medicine (Baltimore)* **2020**, *99* (43), 6, Review. DOI: 10.1097/md.00000000000022955.
- (5) Qi, X. J.; Guo, Z. H.; Chen, Q. Y.; Lan, W. N.; Chen, Z. Z.; Chen, W. M.; Lin, L. Z. A Data Mining-Based Analysis of Core Herbs on Different Patterns (Zheng) of Non-Small Cell Lung Cancer. *Evid.-based Complement Altern. Med.* **2021**, *2021*, 13. DOI: 10.1155/2021/3621677.



- (6) Peng, Z. X.; Wang, Y.; Gu, X.; Wen, Y. Y.; Yan, C. A platform for fast screening potential anti-breast cancer compounds in traditional Chinese medicines. *Biomed. Chromatogr.* **2013**, *27* (12), 1759-1766. DOI: 10.1002/bmc.2990.
- (7) Gao, Y.; Liu, L.; Li, C.; Liang, Y. T.; Lv, J.; Yang, L. F.; Zhao, B. N. Study on the Antipyretic and Anti-inflammatory Mechanism of Shuanghuanglian Oral Liquid Based on Gut Microbiota-Host Metabolism. *Front. Pharmacol.* **2022**, *13*, 15. DOI: 10.3389/fphar.2022.843877.
- (8) Zhang, Y. Z.; Yang, J. Y.; Wu, R. X.; Fang, C.; Lu, H.; Li, H. C.; Li, D. M.; Zuo, H. L.; Ren, L. P.; Liu, X. Y.; et al. Network Pharmacology-Based Identification of Key Mechanisms of Xihuang Pill in the Treatment of Triple-Negative Breast Cancer Stem Cells. *Front. Pharmacol.* **2021**, *12*, 16. DOI: 10.3389/fphar.2021.714628.
- (9) Xu, H. B.; Chen, X. Z.; Wang, X.; Pan, J.; Zhao, Y. Z.; Zhou, C. H. Xihuang pill in the treatment of cancer: TCM theories, pharmacological activities, chemical compounds and clinical applications. *J. Ethnopharmacol.* **2023**, *316*, 20. DOI: 10.1016/j.jep.2023.116699.
- (10) Fu, J.; Zhu, S. H.; Xu, H. B.; Xu, Y. Q.; Wang, X.; Wang, J.; Kong, P. S. Xihuang pill potentiates the anti-tumor effects of temozolomide in glioblastoma xenografts through the Akt/mTOR-dependent pathway. *J. Ethnopharmacol.* **2020**, *261*, 12. DOI: 10.1016/j.jep.2020.113071.
- (11) Chen, Z. H.; Li, Z. M.; Yang, S.; Wei, Y.; An, J. The prospect of Xihuang pill in the treatment of cancers. *Heliyon* **2023**, *9* (4), 14. DOI: 10.1016/j.heliyon.2023.e15490.
- (12) Hu, M. L.; Liao, Q. Z.; Liu, B. T.; Sun, K.; Pan, C. S.; Wang, X. Y.; Yan, L.; Huo, X. M.; Zheng, X. Q.; Wang, Y.; et al. Xihuang pill ameliorates colitis in mice by improving mucosal barrier injury and inhibiting inflammatory cell filtration through network regulation. *J. Ethnopharmacol.* **2024**, *319*, 11. DOI: 10.1016/j.jep.2023.117098.
- (13) Li, X.; Wei, S. Z.; Niu, S. Q.; Ma, X.; Li, H. T.; Jing, M. Y.; Zhao, Y. L. Network pharmacology prediction and molecular docking-based strategy to explore the potential mechanism of Huanglian Jiedu Decoction against sepsis. *Comput. Biol. Med.* **2022**, *144*, 10. DOI: 10.1016/j.combiomed.2022.105389.
- (14) Liu, Z. Y.; Guo, F. F.; Wang, Y.; Li, C.; Zhang, X. L.; Li, H. L.; Diao, L. H.; Gu, J. Y.; Wang, W.; Li, D.; et al. BATMAN-TCM: a Bioinformatics Analysis Tool for Molecular mechANism of Traditional Chinese Medicine. *Sci Rep* **2016**, *6*, 11. DOI: 10.1038/srep21146.
- (15) Wishart, D. S.; Feunang, Y. D.; Guo, A. C.; Lo, E. J.; Marcu, A.; Grant, J. R.; Sajed, T.; Johnson, D.; Li, C.; Sayeeda, Z.; et al. DrugBank 5.0: a major update to the DrugBank database for 2018. *Nucleic Acids Res.* **2018**, *46* (D1), D1074-D1082. DOI: 10.1093/nar/gkx1037.
- (16) Wang, Y.; Yuan, Y.; Wang, W. T.; He, Y.; Zhong, H.; Zhou, X. X.; Chen, Y.; Cai, X. J.; Liu, L. Q. Mechanisms underlying the therapeutic effects of Qingfei Yin in treating acute lung injury based on GEO datasets, network pharmacology and molecular docking. *Comput. Biol. Med.* **2022**, *145*, 20. DOI: 10.1016/j.combiomed.2022.105454.
- (17) Malapelle, U.; Pisapia, P.; Rocco, D.; Smeraglio, R.; di Spirito, M.; Bellevicine, C.; Troncone, G. Next generation sequencing techniques in liquid biopsy: focus on non-small cell lung cancer patients. *Transl. Lung Cancer Res.* **2016**, *5* (5), 505-510, Review. DOI: 10.21037/tlcr.2016.10.08.
- (18) Zhang, Q.; Wang, X. B.; Cao, S. J.; Sun, Y. J.; He, X. Y.; Jiang, B. K.; Yu, Y. Q.; Duan, J. S.; Qiu, F.; Kang, N. Berberine represses human gastric cancer cell growth in vitro and in vivo by inducing cytostatic autophagy via inhibition of MAPK/mTOR/p70S6K and Akt signaling pathways. *Biomed. Pharmacother.* **2020**, *128*, 11. DOI: 10.1016/j.biopha.2020.110245.

- (19) Bekker, G.-J.; Kamiya, N. Advancing the field of computational drug design using multicanonical molecular dynamics-based dynamic docking. *Biophysical reviews* **2022**, *14* (6), 1349-1358, Review. DOI: 10.1007/s12551-022-01010-z.
- (20) Macciò, A.; Oppi, S.; Madeddu, C. COVID-19 and cytokine storm syndrome: can what we know about interleukin-6 in ovarian cancer be applied? *J Ovarian Res* **2021**, *14* (1), 28. DOI: 10.1186/s13048-021-00772-6 From NLM.
- (21) Chatenoud, L.; Ferran, C.; Bach, J. F. The anti-CD3-induced syndrome: a consequence of massive in vivo cell activation. *Current topics in microbiology and immunology* **1991**, *174*, 121-134, Review.
- (22) Jatiani, S. S.; Aleman, A.; Madduri, D.; Chari, A.; Cho, H. J.; Richard, S.; Richter, J.; Brody, J.; Jagannath, S.; Parekh, S. Myeloma CAR-T CRS Management With IL-1R Antagonist Anakinra. *Clin. Lymphoma Myeloma Leuk.* **2020**, *20* (9), 632-+, Editorial Material. DOI: 10.1016/j.clml.2020.04.020.
- (23) Morris, E. C.; Neelapu, S. S.; Giavridis, T.; Sadelain, M. Cytokine release syndrome and associated neurotoxicity in cancer immunotherapy. *Nat. Rev. Immunol.* **2022**, *22* (2), 85-96, Review. DOI: 10.1038/s41577-021-00547-6.
- (24) Mauvais-Jarvis, F.; Klein, S. L.; Levin, E. R. Estradiol, Progesterone, Immunomodulation, and COVID-19 Outcomes. *Endocrinology* **2020**, *161* (9), 8, Review. DOI: 10.1210/endocr/bqaa127.
- (25) Butterworth, M.; McClellan, B.; Allansmith, M. Influence of sex in immunoglobulin levels. *Nature* **1967**, *214* (5094), 1224-1225. DOI: 10.1038/2141224a0.
- (26) Amadori, A.; Zamarchi, R.; De Silvestro, G.; Forza, G.; Cavatton, G.; Danieli, G. A.; Clementi, M.; Chieco-Bianchi, L. Genetic control of the CD4/CD8 T-cell ratio in humans. *Nature medicine* **1995**, *1* (12), 1279-1283, ; Research Support, Non-U.S. Gov't. DOI: 10.1038/nm1295-1279.
- (27) Klein, S. L.; Flanagan, K. L. Sex differences in immune responses. *Nat Rev Immunol* **2016**, *16* (10), 626-638. DOI: 10.1038/nri.2016.90 From NLM.
- (28) Phiel, K. L.; Henderson, R. A.; Adelman, S. J.; Elloso, M. M. Differential estrogen receptor gene expression in human peripheral blood mononuclear cell populations. *Immunol. Lett.* **2005**, *97* (1), 107-113. DOI: 10.1016/j.imlet.2004.10.007.
- (29) Straub, R. H. The complex role of estrogens in inflammation. *Endocr Rev* **2007**, *28* (5), 521-574. DOI: 10.1210/er.2007-0001 From NLM.
- (30) Chen, L. Y. C.; Hoiland, R. L.; Stukas, S.; Wellington, C. L.; Sekhon, M. S. Confronting the controversy: interleukin-6 and the COVID-19 cytokine storm syndrome. *Eur. Resp. J.* **2020**, *56* (4), 7, Editorial Material. DOI: 10.1183/13993003.03006-2020.
- (31) Roux, A.; Xu, Y.; Heilier, J. F.; Olivier, M. F.; Ezan, E.; Tabet, J. C.; Junot, C. Annotation of the Human Adult Urinary Metabolome and Metabolite Identification Using Ultra High Performance Liquid Chromatography Coupled to a Linear Quadrupole Ion Trap-Orbitrap Mass Spectrometer. *Anal. Chem.* **2012**, *84* (15), 6429-6437. DOI: 10.1021/ac300829f.
- (32) Doria, A.; Iaccarino, L.; Arienti, S.; Ghirardello, A.; Zarnpieri, S.; Rampudda, M. E.; Cutolo, M.; Tincani, A.; Todesco, S. Th2 immune deviation induced by pregnancy: The two faces of autoimmune rheumatic diseases. *Reprod. Toxicol.* **2006**, *22* (2), 234-241, Proceedings Paper. DOI: 10.1016/j.reprotox.2006.04.001.
- (33) Gou, Q.; Gong, X.; Jin, J. H.; Shi, J. J.; Hou, Y. Z. Peroxisome proliferator-activated receptors (PPARs) are potential drug targets for cancer therapy. *Oncotarget* **2017**, *8* (36), 60704-60709, Review. DOI: 10.18632/oncotarget.19610.
- (34) Tachibana, K.; Yamasaki, D.; Ishimoto, K.; Doi, T. The Role of PPARs in Cancer. *PPAR Res.* **2008**, *2008*, 15, Review. DOI: 10.1155/2008/102737.
- (35) Fanale, D.; Amodeo, V.; Caruso, S. The Interplay between Metabolism, PPAR Signaling Pathway, and Cancer. *PPAR Res.* **2017**, *2017*, 2, Editorial Material. DOI: 10.1155/2017/1830626.

- (36) Choi, J. M.; Bothwell, A. L. M. The Nuclear Receptor PPARs as Important Regulators of T-Cell Functions and Autoimmune Diseases. *Mol. Cells* **2012**, *33* (3), 217-222, Review. DOI: 10.1007/s10059-012-2297-y.
- (37) Christofides, A.; Konstantinidou, E.; Jani, C.; Boussiotis, V. A. The role of peroxisome proliferator-activated receptors (PPAR) in immune responses. *Metab.-Clin. Exp.* **2021**, *114*, 13. DOI: 10.1016/j.metabol.2020.154338.
- (38) Rosen, E. D.; Sarraf, P.; Troy, A. E.; Bradwin, G.; Moore, K.; Milstone, D. S.; Spiegelman, B. M.; Mortensen, R. M. PPAR $\gamma$  is required for the differentiation of adipose tissue in vivo and in vitro. *Mol. Cell.* **1999**, *4* (4), 611-617. DOI: 10.1016/s1097-2765(00)80211-7.
- (39) Wu, I.; Shin, S. C.; Cao, Y.; Bender, I. K.; Jafari, N.; Feng, G.; Lin, S.; Cidlowski, J. A.; Schleimer, R. P.; Lu, N. Z. Selective glucocorticoid receptor translational isoforms reveal glucocorticoid-induced apoptotic transcriptomes. *Cell Death Dis.* **2013**, *4*, 12. DOI: 10.1038/cddis.2012.193.
- (40) Rhen, T.; Cidlowski, J. A. Antiinflammatory action of glucocorticoids - New mechanisms for old drugs. *N. Engl. J. Med.* **2005**, *353* (16), 1711-1723, Review. DOI: 10.1056/NEJMra050541.
- (41) Martín-Vázquez, E.; Cobo-Vuilleumier, N.; López-Noriega, L.; Lorenzo, P. I.; Gauthier, B. R. The PTGS2/COX2-PGE2 signaling cascade in inflammation: Pro or anti? A case study with type 1 diabetes mellitus. *Int. J. Biol. Sci.* **2023**, *19* (13), 4157-4165, Review. DOI: 10.7150/ijbs.86492.
- (42) Takeuchi, A.; Miyamoto, T.; Yamaji, K.; Masuho, Y.; Hayashi, M.; Hayashi, H.; Onozaki, K. A human erythrocyte-derived growth-promoting factor with a wide target cell spectrum: identification as catalase. *Cancer research* **1995**, *55* (7), 1586-1589, ; Research Support, Non-U.S. Gov't.
- (43) Badawy, M. T.; Sobeh, M.; Xiao, J. B.; Farag, M. A. Androstenedione (a Natural Steroid and a Drug Supplement): A Comprehensive Review of Its Consumption, Metabolism, Health Effects, and Toxicity with Sex Differences. *Molecules* **2021**, *26* (20), 16, Review. DOI: 10.3390/molecules26206210.
- (44) Pang, Q. L.; Jia, A. Y.; Al Masri, M. K.; Varkaneh, H. K.; Abu-Zaid, A.; Gao, X. The effect of androstenedione supplementation on testosterone, estradiol, body composition, and lipid profile: a systematic review and meta-analysis of randomized controlled trials. *Horm.-Int. J. Endocrinol. Metab.* **2022**, *21* (4), 545-554, Review. DOI: 10.1007/s42000-022-00385-8.
- (45) Bian, X. L.; Liu, R.; Meng, Y.; Xing, D. M.; Xu, D. Q.; Lu, Z. M. Cancer Focus Lipid metabolism and cancer. *J. Exp. Med.* **2021**, *218* (1), 17, Review. DOI: 10.1084/jem.20201606.
- (46) Agarwal, D. S.; Krishna, V. S.; Sriram, D.; Yogeewari, P.; Sakhuja, R. Clickable conjugates of bile acids and nucleosides: Synthesis, characterization, in vitro anticancer and antituberculosis studies. *Steroids* **2018**, *139*, 35-44. DOI: 10.1016/j.steroids.2018.09.006.